

# **Comparison between structural properties of bulk GaN grown in liquid Ga under high N pressure and GaN grown by other methods**

Z. Liliental-Weber, J. Jasinski and J. Washburn  
Lawrence Berkeley National Laboratory 62/203, Berkeley, CA 94720

## Abstract

In this paper defects formed in GaN grown by different methods are reviewed. Formation of particular defects are often related to the crystallographic direction in which the crystals grow. For bulk crystals the highest growth rates are observed for directions perpendicular to the c-axis. Threading dislocations and nanopipes along the c-axis are not formed in these crystals, but polarity of the growth direction plays a role concerning defects that are formed and surface roughness. For growth of homoepitaxial layers, where growth is forced to take place in the c-direction threading dislocations are formed and their density is related to the purity of constituents used for growth and to substrate surface inhomogeneities. In heteroepitaxial layers two other factors: lattice mismatch and thermal expansion mismatch are related to the formation of dislocations. Doping of crystals can also lead to formation of defects characteristic for a specific dopant. This type of defects tends to be growth method independent but can depend on growth polarity.

## 1. Introduction

Gallium nitride and related III-V nitrides are promising semiconductors which have applications in both optical devices including light emitting diodes and laser diodes for the blue and UV wavelength region, and electronic devices operating at high temperature, high frequency and high power [1]. The recent commercial realization of light emitting diodes and lasers using III-V nitrides has promoted much more attention in this field of research. Since large size GaN substrates are not commercially available, heteroepitaxial techniques are mostly applied using SiC or sapphire ( $\text{Al}_2\text{O}_3$ ) as substrates. Advances in GaN growth have been achieved using mostly metal-organic chemical vapor deposition (MOCVD) and hydride vapor phase epitaxy (HVPE) for the crystal growth. Molecular beam epitaxy (MBE) is also a suitable technique for the fabrication of high quality device structures using III-V nitrides due to the precise controllability of atomic order, thickness, interface abruptness and composition but its relatively low growth rate compared to other techniques means that this technique is used only for special applications.

Even though recent progress has greatly improved the crystal quality of GaN films grown on various substrates, its practical application is still hampered by a high defect density and by difficulty in p-type doping. In order to control defect formation, it is essential to understand the mechanisms of formation and the detailed structure of particular defects.

In this paper characteristic defects in GaN grown using MOCVD, HVPE and MBE methods on different substrates will be compared to those found in bulk GaN crystals grown from a dilute solution of atomic nitrogen in liquid gallium in the temperature range of 1500K-1800K under high nitrogen pressure up to 20 kbars [2]. Defects formed in layers grown by MOCVD and HVPE on bulk substrates will also be discussed. The influence of growth polarity on formation of particular defects and the effect of introducing Mg, in order to obtain p-doped material in bulk material and in layers grown by MOCVD will also be briefly reviewed.

## 2. Bulk GaN crystals

Bulk GaN is grown from a solution of atomic nitrogen in liquid gallium under high nitrogen pressure (up to 20 kbars) in the temperature range, (1500 -1800 K). Application of high pressure allows crystallization of GaN at the cooler side of the crucible [3].

Bulk GaN grown by this technique crystallizes in the form of platelets or rod-like crystals, but only platelet crystals will be reviewed here. X-ray studies using (004) Cu  $K\alpha$  reflection of the plate-like crystals show the high quality of these crystals with an x-ray rocking curve full-width at half maximum (FWHM) of about 20-30 arc sec for crystals not larger than 1 mm and only slightly broader for larger crystals. By comparison for epitaxial GaN grown on SiC, the x-ray rocking curves have a FWHM of 2.5-4 arc min, and for GaN grown on sapphire of 6-15 arc min [4].

The GaN bulk crystal platelets had the shape of elongated hexagons and had crystallized with a wurtzite structure. The longest axis was frequently along  $[11\bar{2}0]$ . In some cases the samples were less elongated and the dimensions along  $[11\bar{2}0]$  and  $[1\bar{1}00]$  were similar, but in all cases the smallest dimension was in the c-axis direction. The ratio of plate length to thickness along the c axis was typically as large as 100. This shows that growth in the c axis direction is the most difficult. The largest platelets have a size slightly more than 1 cm. When these undoped crystals were studied in cross-section by Transmission Electron Microscopy (TEM) [5] it was observed that one side of the plate was almost

atomically flat while the opposite side was rough (Fig. 1a). Using Convergent Beam Electron Diffraction (CBED) it was determined that the side growing with N polarity had the smooth surface. Growth polarity was also shown to have an important effect on defect formation. The crystal near the side of the plate with the flat surface was structurally perfect, with no extended defects present. In contrast, many planar defects were observed close to the rough surface (the opposite side to the flat surface). These planar defects were stacking faults often associated with dislocation loops decorated by Ga precipitates (Fig. 1b and 2a,b). These stacking faults are nucleated on c-planes during crystal growth by growth mistakes and were observed through the entire length of crystals, therefore it was impossible to observe the partial dislocations at their ends even when more TEM cross-section samples were prepared from one crystal.

There are three possible types of stacking fault in the wurtzite structure which differ by their formation energy: ( $I_1$ ), ( $I_2$ ) and (E) as described in [6]. All these three types of stacking faults were found in the bulk GaN crystals. Formation of a stacking fault in a wurtzite structure can be described as insertion of a sphalerite unit cell which requires rotation of the bonds e.g. the mirror symmetry for bond arrangement typical of the wurtzite structure is lost and it is locally converted to the zinc blende bond arrangement where bonds are rotated  $60^\circ$  with respect to the nearest neighbor bonds. It was found that faults with the higher energy were often associated with extrinsic dislocation loops located on the atomic layer next to such a high-energy stacking fault (Figs. 1b and 2b). This arrangement of an extrinsic dislocation loop in the vicinity of the stacking fault is energetically favorable, because insertion of the additional layer (aA on Fig. 3) converts locally the high-energy fault into a low-energy type of fault (e.g. E-type fault into  $I_1$  type fault shown schematically on Fig.3). The strain field at the surrounding edge dislocation core then helps to nucleate excess Ga precipitation (Figs. 1b,c and 2a,b), since all bulk crystals are grown in an atmosphere of excess Ga. These precipitates were identified by energy dispersive x-ray spectroscopy (EDX). These precipitates were truncated on specific crystallographic planes with a void always located at the upper part of the precipitate for growth with N-polarity (see Fig 1c with the atom arrangement shown on Fig.1a). The fact that these precipitates melted when the electron beam was focused on them is also in agreement with the low melting temperature of Ga.

Growth of bulk GaN platelets takes place mainly at right angles to the c-axis, therefore planar defects formed on the c-planes are the most typical defects in this material. These defects do not propagate into layers grown on top of them.

### 3. Defects in homoepitaxial layers

Three types of crystals will be described in this section: two grown homo-epitaxially using MOCVD and HVPE methods on bulk platelets with Ga or N polarity and the third free-standing GaN crystals grown by HVPE on sapphire substrates to a thickness of at least  $300\ \mu\text{m}$  which had been removed from the substrate by laser lift-off. Such crystals were mechanically polished and dry etched to obtain a smooth epi-ready top surface.

#### 3.1. Defects in MOCVD layers grown on bulk crystals

CBED studies showed that the MOCVD layers retain the polarity of the substrate. However, growth on  $[0001]$  and  $[\bar{0}001]$  GaN surfaces is not equivalent from the point of view of properties of the homoepitaxial layer. The layer quality and type of defects present in the layer depend strongly on the growth polarity. In the epi-layer grown on the “smooth” surface (N-polarity) threading dislocations and inversion domains were found (Fig. 4a). In most cases the threading dislocations started either from

dislocation loops formed at the interface or at some small crystalline island present on this surface, from which several threading dislocations originated. The estimated density of threading dislocations was about  $5 \times 10^6 \text{cm}^{-2}$ . Inversion domains also started from dislocation loops and their density was approximately  $5 \times 10^5 \text{cm}^{-2}$ . Formation of pinholes with walls on (10 $\bar{1}$ 1) planes on the top of inversion domains was also observed. Dislocation loops were also observed in the layer grown with N-polarity probably due to some local inhomogeneities.

For the layer grown on the rough surface (Ga-polarity) no threading dislocations were observed. The interface between the substrate and the layer was not easily visible suggesting a very good continuation of growth in the layer. However, a high density of pinholes (in the range of  $10^6$ - $10^7 \text{cm}^{-2}$ ) was observed in these samples (Fig. 4b). Some pinholes originated at the interface and might indicate places where nucleation of GaN was difficult, possibly related to some contamination at the interface [7].

In both cases this was direct growth, without a buffer layer. Growth with N polarity on the smooth surface was much more difficult to start since decomposition of the substrate tended to take place. It has been found that a N-polar surface decomposes faster and initiation of the growth has to be done at lower temperature than in the case of growth with Ga-polarity. This may explain why dislocation loops were formed at the interface which resulted in the formation of threading dislocations or inversion domains.

### 3.2. HVPE layers grown on bulk crystals

First results for growth of epitaxial layers on bulk GaN using the HVPE technique have been obtained (Fig. 5). For growth with both polarities abrupt interfaces were observed. The big difference was in the growth rate for the two polarities and in the surface smoothness. Growth with Ga polarity was three times faster than growth with N polarity, however, in the later case the surface was more smooth. Formation of some dislocation loops for growth with N polarity was also observed, as was the case for growth using the MOCVD technique but no threading dislocations were formed.

### 3.3. Defects in the “free-standing” HVPE GaN

The free -standing GaN substrates were grown with Ga polarity [8]. Generally such layers grew without any inversion domains propagating to the sample surface; the inversion boundaries coalesced and were overgrown for larger layer thickness. Therefore, they did not have a negative impact on the layer top surface. The main defects in these substrates were dislocations. The majority of dislocations had either mixed or screw character with a density in the range of  $5 \times 10^6 \text{cm}^{-2}$ . The MOCVD homoepitaxial layers grown on top of these free-standing layers were of high crystal quality; one could not even distinguish an interface with the free-standing substrate. The dislocation density was similar to that in the free-standing substrate.

## 4. Heteroepitaxial layers

GaN layers were grown either on SiC or Al<sub>2</sub>O<sub>3</sub> (sapphire) substrates using the MOCVD method. Usually a two step growth was applied with growth of a buffer layer (mostly AlN for growth on SiC and low-temperature GaN for growth on sapphire), followed by the main layer grown at higher temperature.

#### 4.1 Defects in MOCVD layers grown on sapphire

The density of dislocations in the buffer layer is typically very high in the range of  $10^{10}$  to  $10^{11}$   $\text{cm}^{-2}$ . The growth usually starts as islands which finally coalesce to form a continuous layer. Many dislocation half-loops are observed in the buffer layer and in the main layer in the area just above the buffer [9]. The density of dislocation decreases as the layer is grown thicker, but for layers about  $2\mu\text{m}$  thick the density of dislocations at the surface is still in the range of  $10^8$ - $10^9$   $\text{cm}^{-2}$ . The main defects observed in such layers are dislocations, nanopipes, pinholes and occasionally inversion domains. The majority of dislocations are edge type with Burgers vectors at  $90^\circ$  to the c-axis.

Both pinholes and nanopipes start from the V-defect formed on  $(10\bar{1}1)$  planes with about  $56^\circ$  between the V arms. Only some of them develop into long empty nanopipes which either extend to the sample surface or terminate within the layer (Fig. 6). Some nanopipes line up along screw dislocations, but others are not related to any dislocation. The usual diameter of a nanopipe in GaN is observed to be in the range of 2-40 nm, but pinholes can extend in diameter at the sample surface to a few hundred nanometers (300-800 nm). Both types of defects may have the same origin, a nanopipe may develop from what is originally a pinhole and extend for long distances along the c-axis. Both defects can terminate within the layer or extend to the layer surface. Their presence is also independent of the growth method and the substrate used for growth. It is believed that both these defects are impurity related [10].

#### 4.2. Defects in HVPE layers grown on sapphire

Growth of GaN using HVPE is much faster than the growth rate using the MOCVD method, therefore, larger layer thickness can be grown in a shorter time. By growing thicker layers more interaction between dislocations can take place which leads to a smaller density of dislocations. For thin layers of the order of 1-2  $\mu\text{m}$  the density of dislocations is in the range  $2$ - $4 \times 10^9$   $\text{cm}^{-2}$ , similar to that observed in MOCVD layers [11]. However, when a layer grows thicker the number of dislocations near the top decreases to  $1 \times 10^8$   $\text{cm}^{-2}$  for a layer  $55 \mu\text{m}$  thick, and to about  $5 \times 10^6$   $\text{cm}^{-2}$  for a layer thickness of  $300 \mu\text{m}$  (Fig. 7). Interaction between dislocations takes place at the greatest rate in the area close to the interface with the substrate where more dislocations with inclined line directions to the c-axis are present. This is in agreement with the earlier model described by Mathis et al [12]. As the layer becomes thicker this leaves primarily dislocations with line direction along the c-axis and with larger separations between them. Therefore, interaction between dislocations becomes less and less likely and further decrease of dislocation density becomes difficult. Our earlier studies showed that for layer thickness up to  $300 \mu\text{m}$  a decrease of dislocation density took place, which fits a model: inverse proportionality of dislocation density to film thickness, proposed earlier for cubic crystals [13].

All three types of dislocations (screw, edge and mixed) in approximately the same density were observed near the interfaces, but for the thicker layers grown by HVPE a majority of remaining dislocations were either screw or mixed type. For the  $5.5 \mu\text{m}$  layer thickness, the numbers of edge and screw dislocations was similar, while the number of mixed dislocations was about two times higher. A larger fraction of mixed dislocations was also found in the thicker HVPE layer including free-standing layers. A high number of pinholes (voids) seen in cross-sectioned samples as triangles aligned along screw dislocations forming a bamboo-like structure was present in the HVPE layers (Fig.8a). In plan-view configuration these voids had a hexagonal shape. Their formation can be related to the core structure of a screw dislocation or to the higher impurity level in these layers. It appears that this type of defects is the same as pinholes and nanotubes formed in MOCVD layers and confirms earlier

suggestions that they are formed due to impurity accumulation on the low growth rate (10 $\bar{1}1$ ) planes [10].

#### 4.2. Defects in MBE and MOCVD layers grown on top of the HVPE layers

Defects formed in Ga-rich MBE layers grown on top of the HVPE layers showed that dislocations present in the HVPE layer propagate into the newly grown MBE layer. Since these were Ga-rich layers small Ga droplets (precipitates) were found on the sample surface as well as inside the layer, like those observed in the bulk platelets (Fig. 9). In our samples the distribution of these droplets was rather random and not particularly associated with screw dislocations as suggested earlier [13]. There were no pinholes found along the screw dislocations suggesting that these layers had lower impurity content as expected from MBE growth or that core structure of screw dislocations in the Ga-rich MBE layer is different than in the HVPE layer, as suggested earlier [13]. Our high resolution TEM studies of dislocation core structure are in progress to determine if core structure changes in Ga-rich MBE layers.

Similar observation were made for the layers grown by MOCVD on the HVPE substrates. Only dislocations from the top surface of the underneath layer propagated into the top layer. We showed that despite the fact that pinholes were present along screw dislocations in HVPE layers that they were not found in the MOCVD layer grown on top of it (Fig. 8b,c).

### 5. Mg doped GaN

In order to apply GaN as a device material p-n junctions need to be formed. Usually GaN is grown with n-conductivity and p-doping is rather difficult. The most commonly used p-dopant is Mg, however higher hole concentration can be obtained only after thermal annealing [15] in order to dissociate Mg-H complexes. Material made using this process has been used to fabricate light emitting diodes (LEDs) and lasers [1]. Despite this success, many aspects of Mg-doping in GaN are not understood. In the following section defects formed in Mg doped bulk crystals and in layers grown by MOCVD will be compared.

#### 5.1. Defects in bulk GaN:Mg

Bulk Mg doped GaN crystals were grown by the High Nitrogen Pressure Solution Method [2] from a solution of liquid gallium containing 0.1 - 0.5 at.% Mg [15]. The growth solution was homogenized at a temperature of 1100°C for several hours before crystal growth. Then the temperature was increased to the growth temperature (1500 - 1600°C), and a N<sub>2</sub> pressure of 15 kbars was applied for 100 - 150 hours. Crystals in the form of hexagonal platelets approximately 80  $\mu$ m thick and up to 8 mm across were formed. The crystals were approximately the same size and shape as the undoped crystals grown under the same conditions, showing that Mg does not strongly influence the relative growth rates on different crystallographic planes. However, the platelets with Mg were generally somewhat thicker than the undoped samples, which suggests that Mg increases the relative growth rate in the c-direction to some extent. The crystals were either colorless or slightly orange. P-type conductivity was not achieved despite a high concentration of the dopant ( $6 \times 10^{19}$  cm<sup>-3</sup>). All crystals were highly resistive.

We found that the growth polarity characteristics change in comparison with undoped crystals. A “saw-like” surface with a ca. 10 nm roughness was observed on the (000 $\bar{1}$ ) N-polarity side. The surface for the opposite growth direction was flat with only occasionally one- or two atomic step terraces [17-

19]. Under certain growth conditions, Mg was found to cause the formation of different types of defects depending on the growth polarity. For growth with N-polarity, planar defects, Mg-rich, form a superlattice-like array typical for polytypoids, which are most probably thin (not more than two unit cells) inversion domains formed on the c-planes separated by perfect GaN with a repetition period of 10 nm (Fig. 10a) [17-19].

Growth with Ga polarity leads to formation of pyramidal defects, pinholes, empty inside (Fig. 10b). The dimension of the largest defects are in the range 100 nm (measured length of their bases) and the smallest about 3-5 nm. The density of these defects is about  $2.5 \times 10^9 \text{ cm}^{-2}$ . They appear in [11 $\bar{2}$ 0] cross-section TEM micrographs as triangular features. All of these triangles were oriented in a direction with the base plane closer to and parallel to the sample surface with Ga-polarity, e.g. from the triangle tip to the base the bond direction along the c-axis is from Ga to N. Study in plan-view configuration confirms that these defects are pyramids and they are empty inside with a segregation of Mg on the defect base formed on the c-plane as well as on the inclined surfaces. This shows that these defects are not inversion domains as suggested earlier [20].

Based on the measurement of the layer thickness containing a particular type of defect one can compare the growth rate for Mg doped bulk GaN crystals for opposite crystal polarities. Such measurements show that the growth in the direction with N-polarity is at least one order of magnitude smaller than growth in the direction with Ga-polarity for these doped crystals.

## 5.2. Defects in MOCVD GaN:Mg

Planar defects similar to these found in bulk material were also found in Mg-delta doped MOCVD grown crystals [17-19] where 130-periods of GaN:Mg delta doped superlattice was grown at 1030 °C. 106 Å-thick layers of GaN, were each followed by a 15 second exposure of Cp<sub>2</sub>Mg. During the Cp<sub>2</sub>Mg exposure, the TMGa was vented, but the NH<sub>3</sub> and H<sub>2</sub> remained flowing into the chamber. This was in order to verify if the ordered structure of planar defects formed in bulk GaN crystals could be grown by another technique. The study showed that the planar defects are observed only for several of the first delta doped layers. Further growth of delta doped layers did not result in planar defect formation, but rather in formation of pyramids characteristic for the bulk growth with Ga polarity. In the area where the planar defects were formed a higher Mg concentration was observed using SIMS measurements [19]. When Mg was continuously added during the growth only the pyramidal defects were formed, no planar defects were observed in such samples.

## 6. Summary and Conclusions

This review of defects formed in GaN grown using different methods shows that the kind of defect which is formed depends on the crystallographic growth direction and on growth polarity. For bulk crystals where growth proceeds primarily along [11 $\bar{2}$ 0] or [11 $\bar{0}$ 0] directions, planar defects on c-planes dominate. In bulk crystals c-axis threading dislocations and nanotubes were not found, but the surface morphology changed drastically with different growth polarity.

When homoepitaxial layers are grown by MOCVD on bulk substrates then the crystal is forced to grow in the c-axis direction and the growth rate depends on the growth polarity. Impurities, substrate surface inhomogeneities or substrate decomposition can lead to the formation of threading dislocations, inversion domains, nanopipes and pinholes, similar to those observed in heteroepitaxial layers. The density of these defects in homoepitaxial layers can be negligible for well prepared substrate surfaces, but locally these defects may appear if any inhomogeneities (such as polishing damage) is be present.

Formation of nanopipes and pinholes appears to be related to the purity of the constituents used for growth, but growth polarity plays a role as well, since slower growth rate allows exposure of a particular surface to a particular impurity for longer times.

The use of HVPE growth which permits a higher growth rate appears promising despite the fact that this growth technique on bulk substrates is in an early stage of development. No interfacial defects were found for growth in either crystal polarity. Occasionally small dislocation loops were found in the homoepitaxial layers like in bulk material.

In heteroepitaxial films, due to the growth on substrates with different lattice parameters than the layer, a high density of misfit dislocations are formed and the interaction between them leads to the formation of threading dislocations. These defects are formed due to the lattice mismatch and the difference in thermal expansion coefficients between the substrate and the epilayer. Substrate surface inhomogeneities also play a similar role as in the homoepitaxial layers. Since HVPE growth allows larger layer thickness, more interaction between threading dislocations can take place leading to substantial decrease of threading dislocation density in the thick layers. However, crystals grown by this method will never be dislocation free. Growth to large thickness can also lead to crack formation, not discussed in this paper.

Nanotubes and pinholes are also formed in heteroepitaxial layers and their density is related most probably to the level of certain impurities. However, any nanopipe or pinhole can be overgrown and closed in a clean environment since growth along the c-planes will be faster than along c-direction.

Doping of a GaN crystal by Mg leads to the formation of defects that are different for the two growth polarities. For growth with N polarity planar defects are formed but for the growth with Ga polarity small pyramids with a hexagonal base on the c-plane and inclined(11 $\bar{2}$ 3) surfaces are formed. The surfaces of these defects are Mg rich and their size will differ for different growth rates. For the bulk crystals where growth is extremely slow large defects are formed but the same defects are much smaller when the MOCVD growth method is used. These defects are empty inside. This suggests that when a (11 $\bar{2}$ 3) surface is covered by Mg further growth does not take place and small pinholes with Mg rich walls are formed. Formation of these defects is not growth method dependent.

However formation of some defects like pinholes is growth method specific. For example, in HVPE films pinholes arranged on top of each other are formed along screw dislocation cores. However, if MBE is then used to grow additional material on top of this HVPE layer, these defects are not formed. This is probably related to different purity of these materials when grown by the different methods. High resolution electron microscopy with subangstrom resolution is in progress to study the cores of screw dislocations in order to find the explanation for these differences.

## Acknowledgment

This work was supported by the U.S. Department of Energy under the contract No. DE-AC03-76SF00098. The use of the facility at the National center for Electron Microscopy at the LBNL is greatly appreciated. The authors want to thank Drs. S. Porowski, I. Grzegory, J. Baranowski, R. Dupuis, R. Molnar, H. Morkoc and S.S. Park for providing GaN samples.

## References:

1. S. Nakamura and G. Fasol, "The Blue Laser Diode" (Springer, Berlin, 1997).
2. I. Grzegory, J. Jun, M. Bockowski, St. Krukowski, M. Wroblewski, B. Lucznik and S. Porowski, J. Phys. Chem. Solids 56, 639 (1995).

3. S. Porowski, I. Grzegory, and J. Jun in "High Pressure Chemical Synthesis" eds. J. Jurczak and B. Baranowski, Elsevier Science Publishers, B.V. (1989) p. 21.; S. Porowski and I. Grzegory, in "Properties of Group III Nitrides" ed. James H. Edgar, EMIS Data-reviews Series No. 11 (1994), p. 76).
4. M. Leszczynski, T. Suski, P. Perlin, I. Grzegory, M. Bockowski, J. Jun, S. Porowski, and J. Major, *J. Phys. D. Appl. Phys.* 28, A 149 (1995).
5. Z. Liliental-Weber, C. Kisielowski, S. Ruvimov, Y. Chen, J. Washburn, I. Grzegory, M. Bockowski, J. Jun, and S. Porowski, *J. Electr. Mat.* vol. 25, 1545 (1996).
6. D. Hull and D.J. Bacon "Introduction to Dislocations" International Series on materials Science and Technology, vol. 37 (1985) Pergamon International Library, Publisher: R. Maxwell, pp. 112-121.
7. J.M. Baranowski, Z. Liliental-Weber, K. Korona, K. Pakula, R. Stepniewski, A. Wyszomolka, I. Grzegory, G. Novak, S. Porowski, B. Monemar, and P. Bergman, Structural and Optical Properties of Homoepitaxial GaN Layers." *Mater. Res. Soc. Symp.* vol. 449, 393 (1997).
8. J. Jasinski, Z. Liliental-Weber, D. Huang, M.A. Reshchikov, F. Yun, H. Morkoc, C. Sone, S.S. Park, and K.Y. Lee, *Proc. Symp. Mat. Res. Soc.* (2002) in press.
9. S. Ruvimov, Z. Liliental-Weber, H. Amano, and I. Akasaki, "Atomic Structure of Grain Boundaries and Interfaces in III-Nitrides Epitaxial Systems," *MRS Proc.* vol. 482, 387 (1998).
10. Z. Liliental-Weber, Y. Chen, S. Ruvimov, and J. Washburn, "Formation Mechanism of Nanotubes in GaN" *Phys. Rev. Lett.* 79, 2835 (1997).
11. J. Jasinski and Z. Liliental-Weber, *J. Electr. Mat.* 31, (2002) in press.
12. S.K. Mathis, A.E. Romanov, L.F. Chen, G.E. Beltz, W. Pompe, and J.S. Speck, *J. Cryst. Growth* 231, 371 (2001).
13. J.S. Speck, M.A. Brewer, G. Beltz, A.E. Romanov, and W. Pompe, *J. Appl. Phys.* 80, 3808 (1996).
14. J.W.P. Hsu, J. Manfra, S.N.G. Chu, C.H. Chen, L.N. Pfeiffer, and R.J. Molnar, *Appl. Phys. Lett.* 78, 3980 (2001).
15. S. Nakamura, N. Iwasa, M. Senoh, and T. Mukai, *Jpn. J. Appl. Phys.* 31, 1258 (1992).
16. S. Porowski, M. Bockowski, B. Lucznik, I. Grzegory, M. Wroblewski, H. Teisseyre, M. Leszczynski, E. Litwin-Staszewska, T. Suski, P. Trautman, K. Pakula and J.M. Baranowski, *Acta Physica Polonica A* vol., 92, 958 (1997).
17. Z. Liliental-Weber, M. Benamara, J. Washburn, I. Grzegory, and S. Porowski, "Spontaneous Ordering in Bulk GaN:Mg Samples," *Phys. Rev. Lett.* 83, 2370 (1999).
18. Z. Liliental-Weber, M. Benamara, W. Swider, J. Washburn, I. Grzegory, and S. Porowski, :D.J.H. Lambert, C.J. Eiting, and R.D. Dupuis, "Mg-Doped GaN: Similar Defects in Bulk and MOCVD Grown Material" *Appl. Phys. Lett.* 75, 4159 (1999).
19. Z. Liliental-Weber, M. Benamara, W. Swider, J. Washburn, I. Grzegory, and S. Porowski, :D.J.H. Lambert, R.D. Dupuis, and C.J. Eiting, "Ordering in Bulk GaN:Mg Samples; Defects Caused by Mg Doping" *Phys. B* vol. 273-274, 124 (1999).
20. P. Vennegaes, M. Benaissa, B. Beaumont, E. Felton, P. De Mierry, S. Dalmaso, M. Leroux, and P. Gibart, *Appl. Phys. Lett.* 77, 880 (2000).

## Figure Captions:

Fig. 1. (a) TEM cross-section micrograph through bulk GaN platelet indicating different surface roughness; (b) Higher magnification micrograph showing defects observed near the rough side of the crystals: stacking faults (SF) seen edge-on as thin lines observed through the entire crystals, dislocations loops (DL) seen edge-on as short lines with precipitates (P) located on dislocation loops; (c) higher magnification of a dislocation loop with the precipitate (P). Note truncation of the precipitate and void location in the upper part of the precipitate.

Fig. 2. (a) Dislocation loops (DL) decorated by Ga precipitates (P) observed by TEM in plan-view samples; (b) High energy stacking fault with a dislocation loop (DL-darker contrast in the central part of the micrograph) adjacent to the stacking fault (SF) observed in cross-section bulk GaN samples.

Fig. 3 Schematic drawing of the E-type high energy stacking fault (SF) converting to an  $I_1$  low energy stacking fault by inserting aA planes forming a dislocation loop (DL-shaded).

Fig. 4. (a) Defects in the MOCVD grown GaN layer grown with N-polarity. A narrow inversion domain (ID) shown with a darker contrast with a pinhole formed on top of it and two threading dislocations (D) attracted to the pinhole. All these defects started from the dislocation loop (darker contrast). Dark line at the interface between the substrate and the epilayer indicates presence of some type of inhomogeneity; (b) Pinholes formed in the MOCVD GaN layer grown with Ga-polarity on top of bulk GaN.

Fig. 5. Interfaces between HVPE grown GaN layer and the bulk substrate for growth with different polarities: (a) Ga polarity, (b) N polarity. The arrows indicate the interfaces between the bulk substrate and the HVPE layer observed in both samples.

Fig. 6. (a) Nanopipes observed in a MOCVD layer grown with Ga polarity on SiC. Arrows indicate the length of these nanopipes and show that some of them terminate within the crystal and do not propagate to the sample surface; (b) A magnified image of a nanopipe confirming that they originate from the V-defect similarly as a pinhole.

Fig. 7. Dislocation density in the HVPE layers at different layer thicknesses.

Fig. 8. (a) Pinholes along screw dislocation in a HVPE GaN layer. Contrast on the dislocation disappears for this diffraction condition; (b,c) Pinholes along a screw dislocation in the HVPE layer and lack of them in the layer grown on top of it by the MOCVD method; (b) an image taken with the diffraction condition when the screw dislocation is in contrast; (c) the same image with the diffraction condition when the screw dislocation is out of contrast. The arrows in (b) and (c) indicate the expected position of the interface between the HVPE and MOCVD grown layers.

Fig. 9. Formation of a Ga precipitate in the vicinity of a screw dislocation in a Ga-rich MBE layer grown on top of the HVPE layer; (a) and (b) are images of a screw dislocation near the Ga precipitate. These two images show the screw dislocation out of contrast in (a) for  $g=(11\bar{2}0)$  and in contrast (b) for  $g=(0002)$ .

Fig. 10 (a) An array of planar defects formed in bulk GaN:Mg grown with N-polarity; (b) Pyramidal defect formed in the MOCVD crystals grown with Ga polarity. Note expansion between two lattice planes on the base of the defect suggesting that Mg segregates only on the defect walls. Much larger pyramidal defects are formed in bulk GaN crystals.

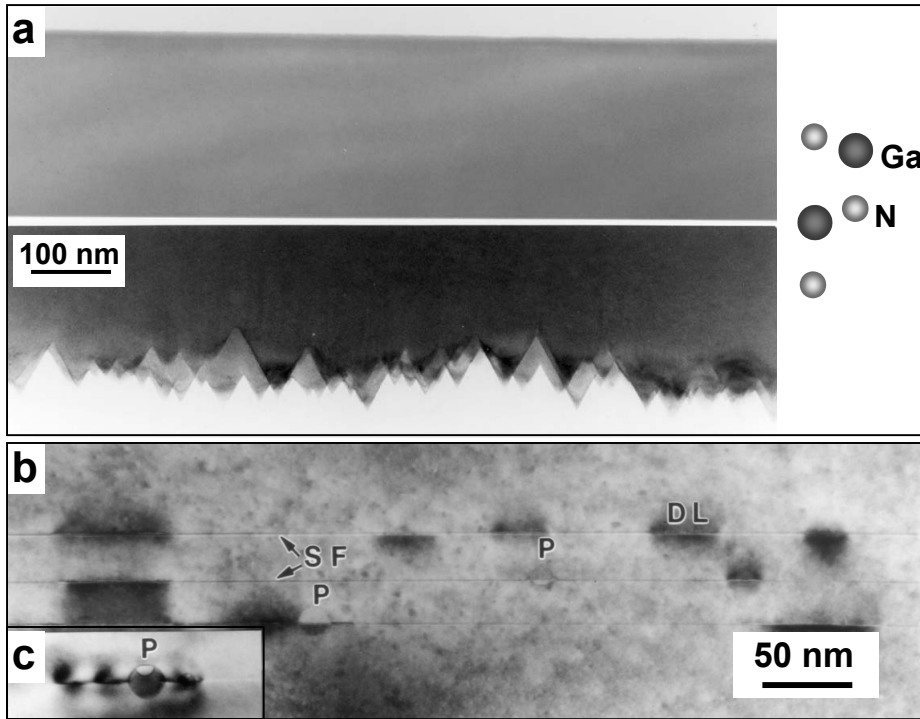


Fig. 1.

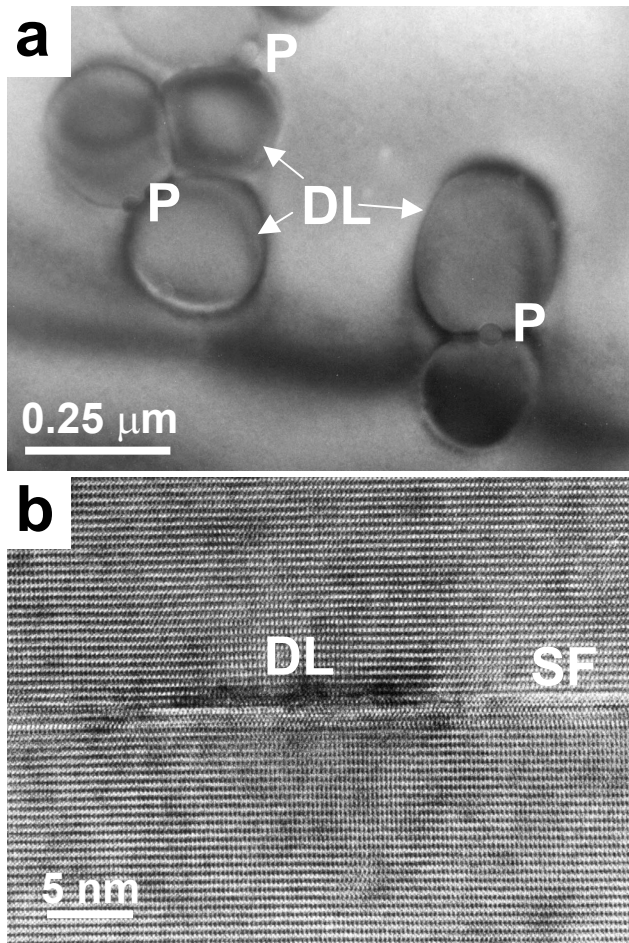


Fig.2

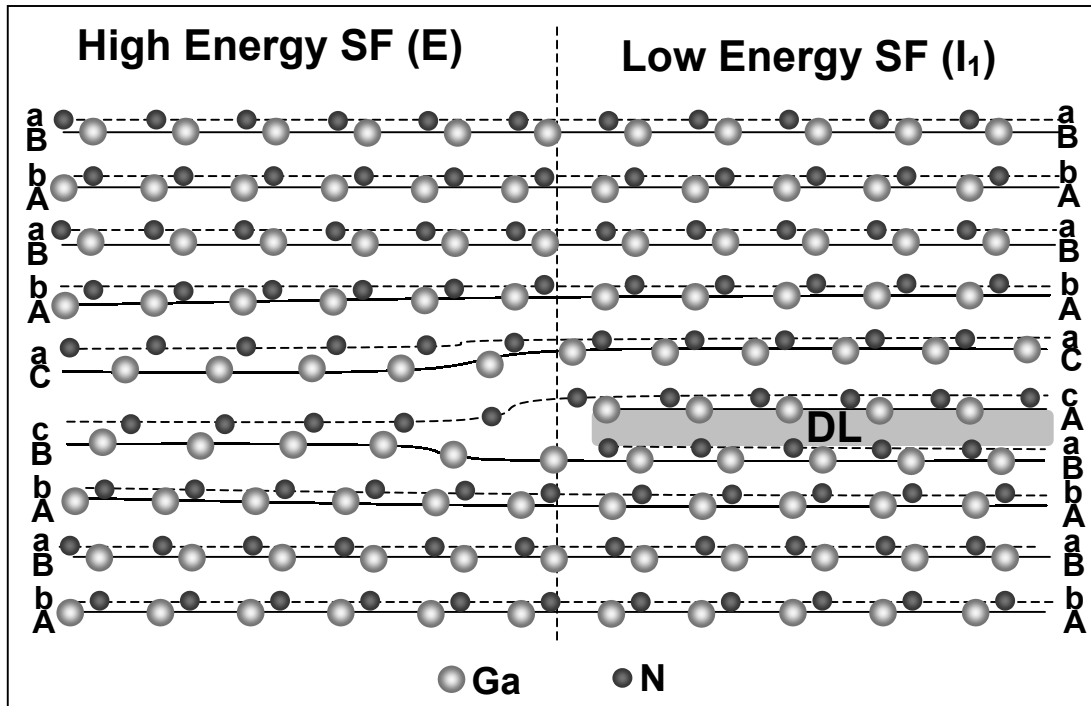


Fig. 3.

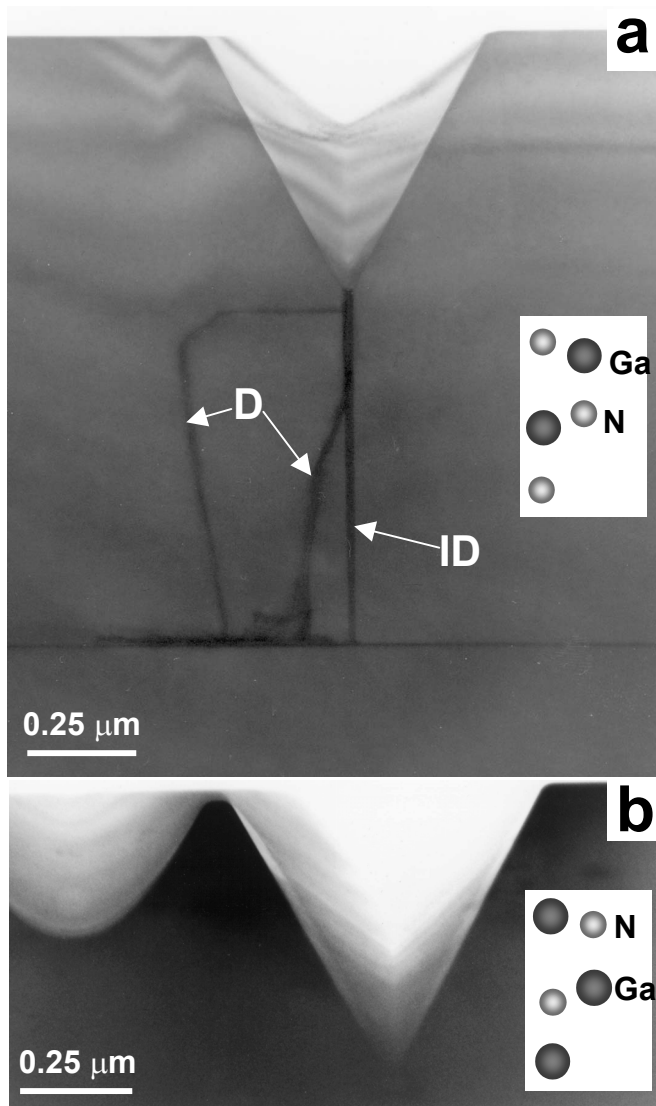


Fig. 4.

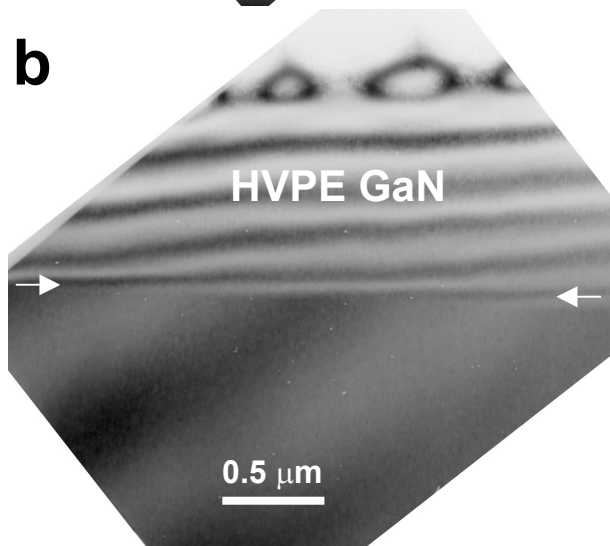
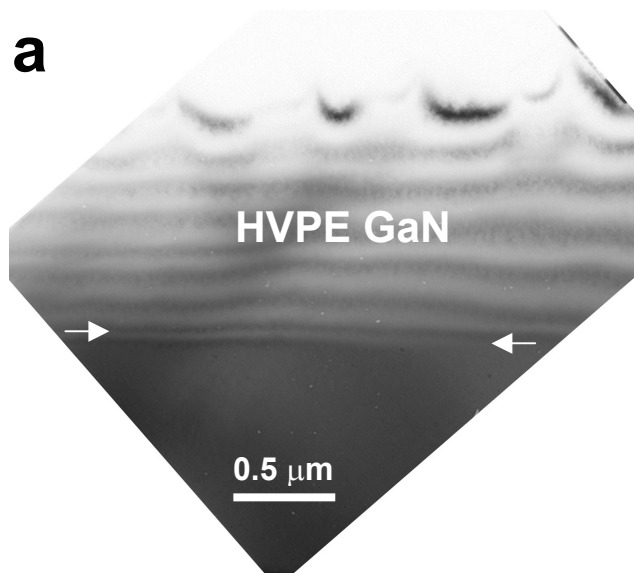


Fig. 5.

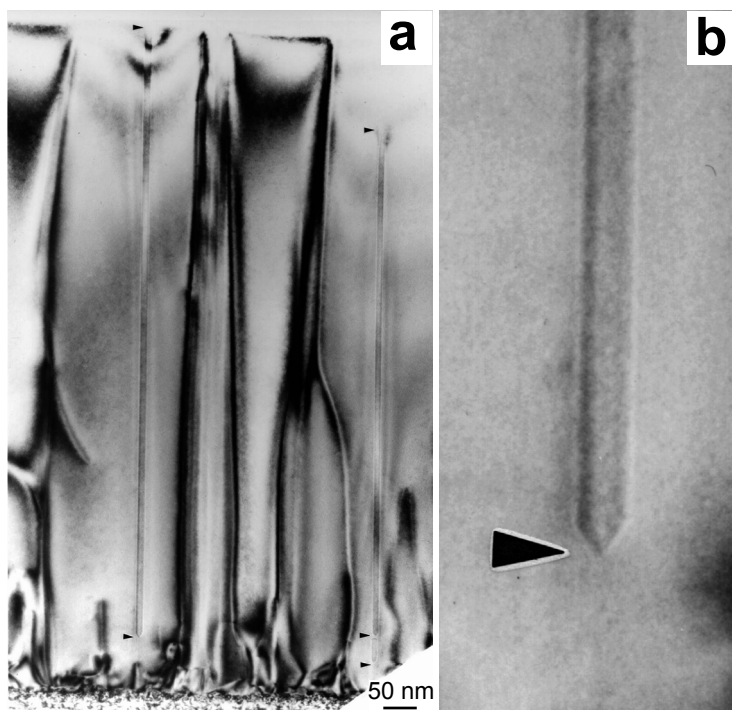


Fig.6.

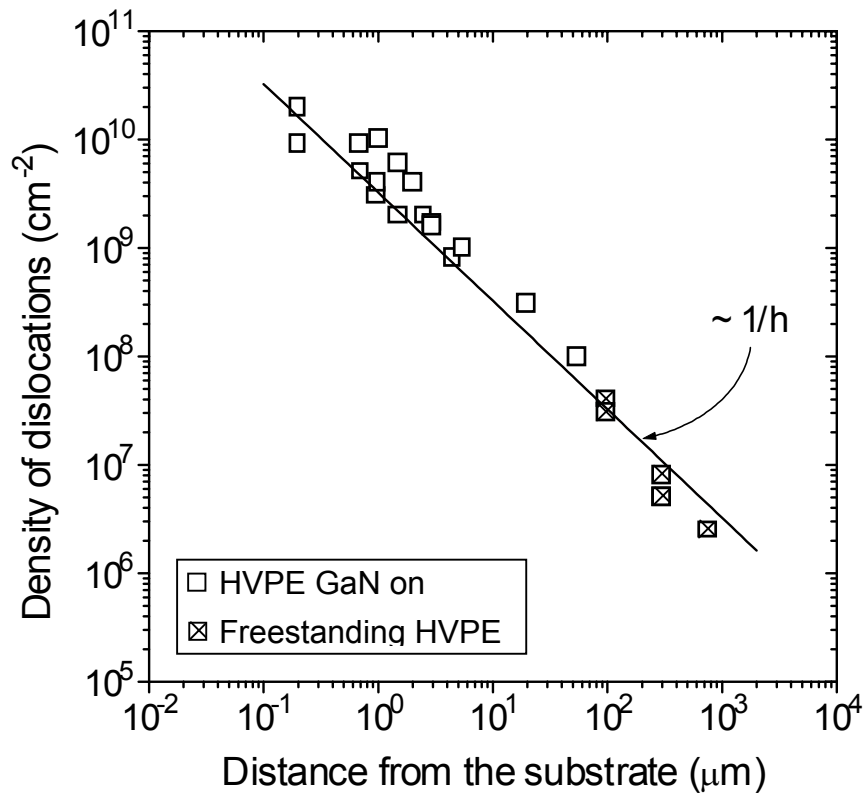


Fig. 7.

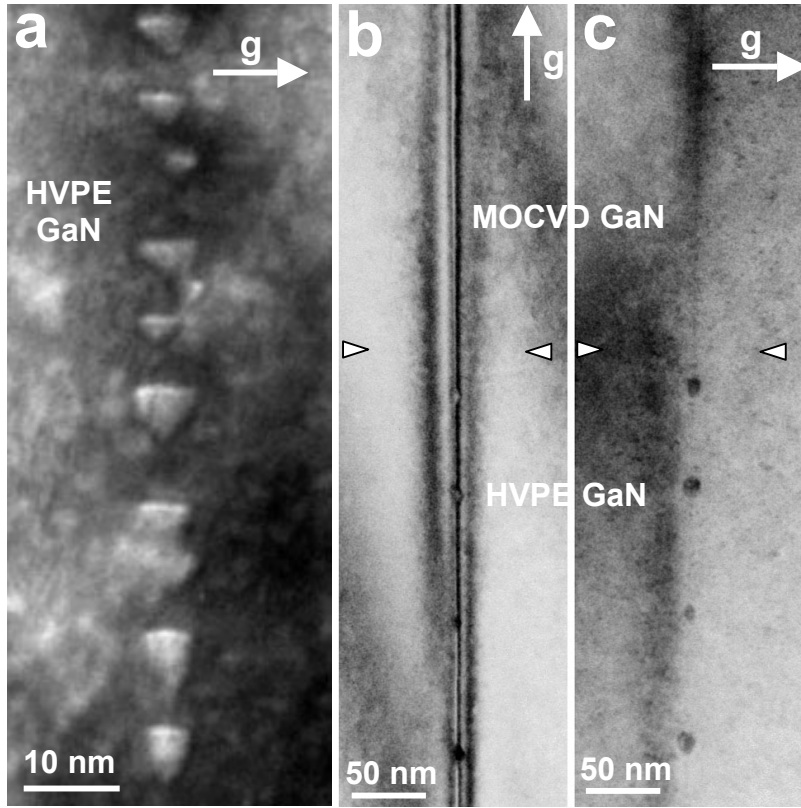


Fig. 8.

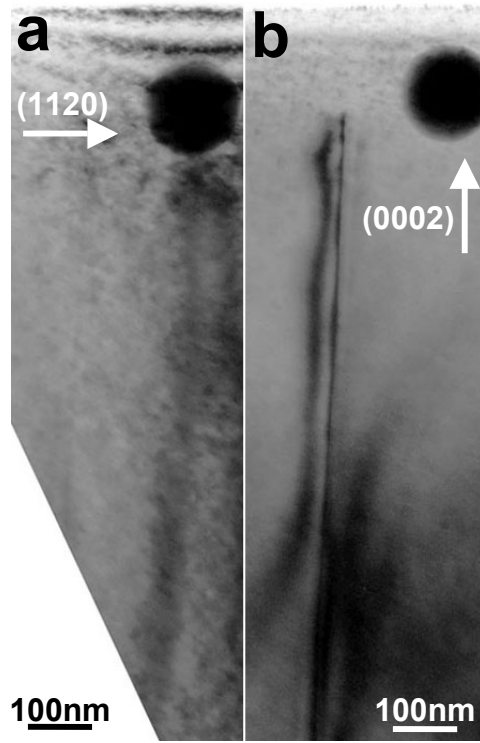


Fig. 9.

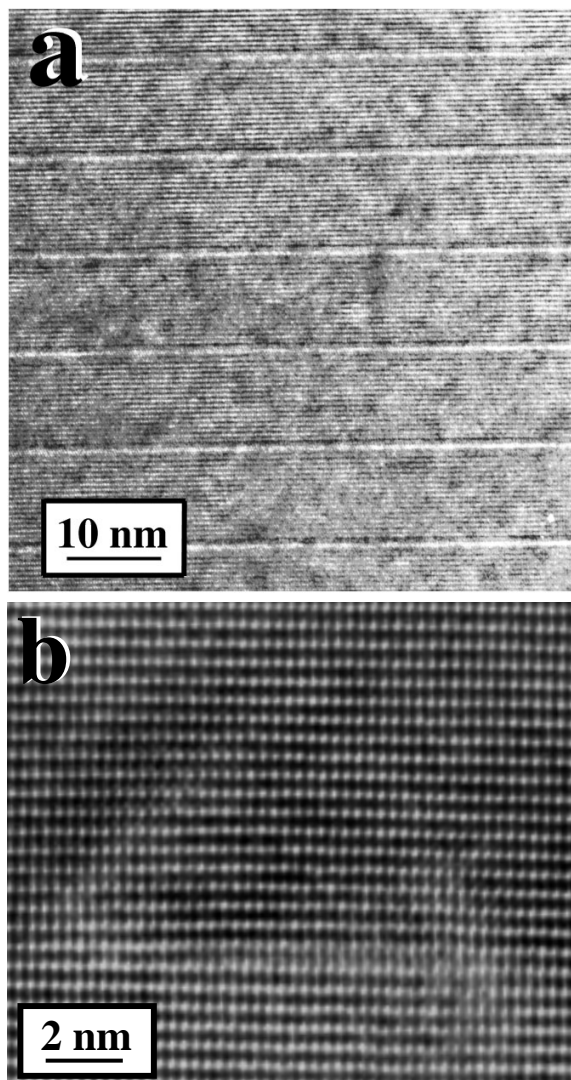


Fig. 10.